Simulating Plasmon Effect in Nanostructured OLED Cathode Using Finite Element Method

Leiming WANG ✳, Jun AMANO ✳, Po-Chieh HUNG ✳

Abstract

Coupling of light to surface plasmons at metal cathode represents a significant light loss in organic light-emitting diode (OLED), resulting in its overall low energy efficiency. In this report, numerical models to simulate the plasmon coupling effect at the metal cathode and to reduce plasmon energy loss by nanostructured cathode are described. The simulation was done in the framework of finite element method (FEM) carried out in a commercial software package (COMSOL Multiphysics). In the electromagnetic wave frequency domain simulation, the molecular emitter is modeled by a classic point dipole driven by continuous electric current, and Ag is selected as the cathode material. The simulation visualizes the light field distribution in a multilayer OLED structure and its coupling to surface plasmon polariton waves (SPP) in real space. Two-layer structure models are then used to quantitatively analyze the percentages of plasmon losses for flat and nanograting cathode structures. The FEM model allows simulation of arbitrary cathode structures and variation of its material properties, and thus enables parametric optimization of the cathode structure and material for minimization of plasmon loss. Our simulation results suggest that ~50 % reduction of plasmon energy loss over a broadband emission is possible by optimized metal cathode structures.

1 Introduction

OLED is an emerging technology for next-generation flat panel display and solid-state lighting due to its many attractive advantages, such as lightweight, low power consumption, thin and flexible form factors. Konica Minolta is one of the leading companies developing and commercializing high luminous efficiency OLED lighting panels.

A typical bottom emitting OLED has a multilayer structure that includes a glass or plastic substrate, a transparent anode (usually indium tin oxide (ITO)), a hole transport layer (HTL), an emitting layer (EML), an electron transport layer (ETL), and a metal cathode, as schematically illustrated in **Fig. 1**. Due to total internal reflections caused by the mismatch in the refractive index between each layer, as well as plasmon coupling loss at metal cathode, typically only about 20 % of the emitted light can leave the device, limiting its light extraction efficiency.[1] Among the many light loss mechanisms, coupling to surface plasmons amounts to about 40 % of the total emitted
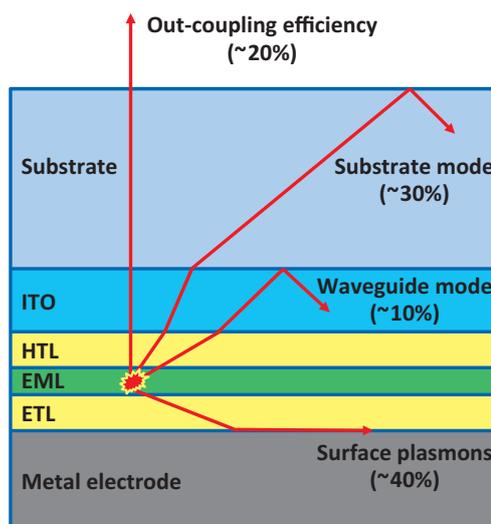

Fig. 1 Schematics of a multilayer OLED structure and various kinds of light out-coupling losses.

✳ Konica Minolta Laboratory U.S.A, Inc.

light, and elimination/reduction of plasmon loss thus represents a big challenge in improving the light extraction efficiency of OLED.

Several approaches have been explored both theoretically and experimentally to reduce the plasmon coupling loss in OLED, such as horizontally orienting the molecular emitters[2], increasing the distance between emission zone to the cathode[3], fabricating metal-free electrode[4], or using nanograting structures[5]. While some of those methods have achieved limited practical successes, non-trivial discrepancies are also seen among different literature. A systematic study of the plasmon coupling mechanism and the structural effect, particularly with subwavelength nanostructured cathode, on the plasmon loss of OLED has been rare. Such effort could be achieved computationally by utilizing electromagnetic wave numerical simulations such as FEM[6] or finite-difference time-domain (FDTD) method[7].

In this paper, we describe a numerical model to simulate the plasmon coupling effect in OLED and to explore the reduction of plasmon loss by nanograting cathode structure. The simulation indicates that plasmon loss is mainly through the coupling of dipole emission into SPP. SPP is a surface wave confined at the ETL/metal cathode interface with its energy being eventually dissipated into the metal electrode. A simplified model of Ag/EML two-layer structure was adopted to quantitatively analyze the percentages of plasmon losses for flat and nanograting cathode structures. The results suggest that plasmon coupling can be significantly reduced by fabricating nanograting structures at the cathode/organic material interface. Parametric studies were also performed to survey the effect of the size, shape, and period of the nanograting on the plasmon loss reduction.

2 Simulation method

The simulation is performed using the RF module of COMSOL Multiphysics. Maxwell's equations are calculated in the frequency domain to simulate the field distribution inside a multilayer material. Since plasmon effect is essentially a near field phenomenon, only near field are calculated. We started with 2D simulations. Fig. 2 (a) shows a schematic of the simulation domain which is 6-layer stack of materials corresponding to those shown in Fig. 1. The thickness of each layer in the simulation is indicated in the figure. The wavelength dependent optical properties (dielectric constant or refractive index) of each material are obtained from either experimental data or literature[8] and are tabulated in the COMSOL FEM model for interpolation. A classic electric point dipole with unit dipole moment is placed at the middle of EML layer to model the molecular emitter in the OLED, as indicated by a red arrow in Fig. 2 (a). This has been shown to be a valid approximation[9].

The horizontal scale of the simulation domain is set as 10 μm, few ten times longer than that of the simulation wavelength in order to reveal the wave behavior of different mode in a propagated distance. All domain boundaries except the bottom of the Ag electrode are surrounded by Perfectly Matched Layer (PML) to absorb outgoing waves. The skin depth of Ag at visible wavelength is about 20 nm, so the transmission through 120 nm Ag film is negligible, and no PML is needed at the bottom boundary. PML at the top boundary assumes infinite half space for glass substrate and the substrate/air interface effect is not included in the simulation, since the substrate in an OLED device is optically thick which cannot be efficiently treated in the FEM computation. Note that
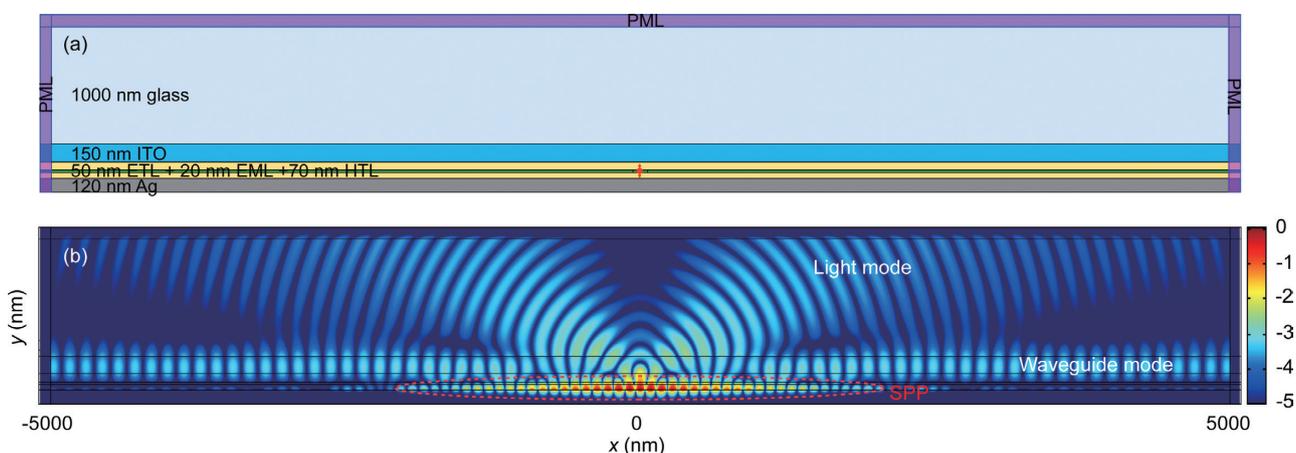

Fig. 2 (a) The 2D simulation domain, and (b) the simulated field distribution of a dipole emission in a multiplayer OLED structure. The field intensity is normalized and plotted on a log color scale.

special care needs to be taken for PML set up at the metal/dielectric interface region for appropriate absorption of the SPP waves. Specifically, the SPP is a decaying wave; a complex number SPP wavelength has to be specified in the PML setting at the Ag/organic layer interface region.

Due to thin film nature of the multi layers, swept mesh is used for all domains, except a small boxed region enclosing the dipole source where free triangular mesh is applied. Convergence test has been performed to ensure the mesh density is sufficient. Finally, the geometrical properties in the COMSOL model are all parameterized to enable structural optimization without re-editing the model geometry.

3　Simulation results and discussion

3. 1　Visualizing the mode distribution in OLED

Fig. 2 (b) shows the field distribution from a 2D simulation of a dipole emission inside a multilayer OLED structure corresponding to Fig. 2 (a). The dipole is vertically oriented (P_y), i.e., perpendicular to the layer interfaces and separated from the Ag surface by 60 nm. The vacuum wavelength (λ_0) of the emission is 475 nm. Fig. 2 (b) is the normalized y-component of the electric field intensity ($|E_y|$). Coupling of the dipole emission into different light modes can be readily identified. For example, the quasi-cylindrical like wave inside the glass corresponds to light mode emitting to the far field. As mentioned above, the glass substrate is treated as infinitely thick in the simulation, so there is no distinguishment between the substrate mode and the air mode. The plane wave like component inside the ITO and the organic layers is recognized as the waveguide mode. As seen in Fig. 2 (b), the waveguide mode propagates essentially

horizontally toward the sides and does not contribute to light emission of the device. Finally there is the component marked by the red dashed line, it features relative high intensity, strong confinement at the metal/dielectric interface region, and quick attenuation of the intensity as it propagates away from the source. Those features are the characteristics of a SPP wave. Hence the simulation reveals the main mechanism of the plasmon loss is excitation of the SPP wave at the cathode interface. To the best of the authors' knowledge, this is the first time that the mode distribution and the plasmon coupling in OLED is visualized in real space.

3. 2　Reducing plasmon loss with nanograting

In this section, we examine the possible reduction of the plasmon coupling by nanograting cathode structure. To focus on the plasmon effect, herein and after we limit our simulation to a simplified Ag/EML 2-layer structure. Fig. 3 displays simulated field distribution ($|E_y|$) of a vertical dipole (P_y) emission ($\lambda_0 = 535$ nm) inside the 2-layer structure comprising of 120 nm Ag and 1500 nm EML material. The dipole is inside the EML material and is 50 nm above the metal surface. Fig. 3 (a) is the field distribution for a flat interface, which shows that for the 2-layer structure the majority of the dipole emission is coupled to the SPP wave, while only a small portion is radiated as free light into the EML as indicated by its much weaker intensity. Fig. 3 (b) shows the result for a 2-layer configuration with nanograting structure at the interface, indicating that the SPP coupling is greatly suppressed in this case. The geometry of the nanograting and its structural parameters are schematically shown in the inset of Fig. 3 (b). For this simulation, dimension of the grating is a period (λ_G) of 100 nm, a pitch
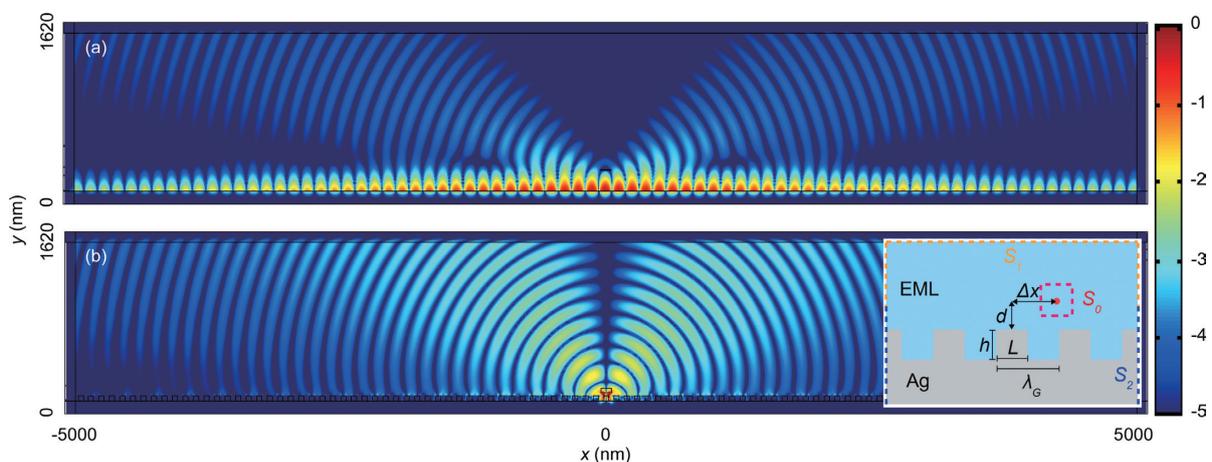

Fig. 3 2D simulated field distribution of a dipole emission in a 2-layer structure with (a) flat, and (b) nanograting interface. The inset in (b) shows schematic of the nanograting with its structural parameters. The field intensity is normalized and plotted on a log color scale.

width (L) of 50 nm, and a pitch height (h) of 50 nm. The dipole is at 50 nm (d) above the center of a pitch ($\Delta_x = 0$). The results suggest that significant reduction of plasmon loss is viable by subwavelength nano-structured cathode.

3.3 3D simulation

OLED is an incoherent light source, in which ensemble of molecular emitters align randomly and emit independently. The overall effect is the average of three dipole orientations: one perpendicular and two parallel to the interfaces of the multi-layers[7]. Therefore, 3D simulation is the most suited to characterize the isotropic nature, while 2D simulation imposes some artificial symmetry (in the z direction) and polarization (s- or p- polarized) on the system. Nevertheless, 2D simulation suffices to illustrate the mechanism of the plasmon loss and to compare between flat and nanograting structures. Here a 3D calculation is performed for crosscheck as presented in **Fig. 4 (a)** and **(b)**. Due to high memory consumption, the 3D simulation is limited to a small domain size as labeled in the figure. The 3D simulation is done for a vertical dipole (P_z) with emission wavelength (λ_0) of 535 nm. The 3D calculations also show that strong SPP excitation occurs in the flat structure indicated by the strong field intensity in the x-y cross section plane at the interface as shown in **Fig. 4 (a)**, while for the nanograting cathode structure shown in **Fig. 4 (b)**, the coupling to SPP is negligible, confirming the results obtained in the 2D simulations.

3.4 Power flow analysis

To quantitatively compare between the flat and nanograting cathode structures for plasmon loss, partition of the total emission power into the light mode and the plasmon mode are calculated in the 2D simulation of the 2-layer system. In the inset of **Fig. 3 (b)**, the color dashed lines denote the boundaries used to integrate the power of each mode. Specifically, power flow (Poynting vector) goes out through the rectangular box enclosing the source (S_0) calculates the total emission power of the dipole. The power flow integrated over boundary S_1 represents the light mode, and that over the S_2 for SPP. Note that S_2 is extended some distance into the EML to account for the evanescent field of SPP. Due to interference between the light mode and SPP, this extended distance is somewhat arbitrary. In the simulation, it is selected as the distance to where the SPP field intensity decays to e^{-1} relative to that at the interface. In addition, the

power of plasmon mode also needs to include the resistive loss in the metal, since SPP is a lossy wave and part of its energy is dissipated inside the metal before it reaches the domain boundary.
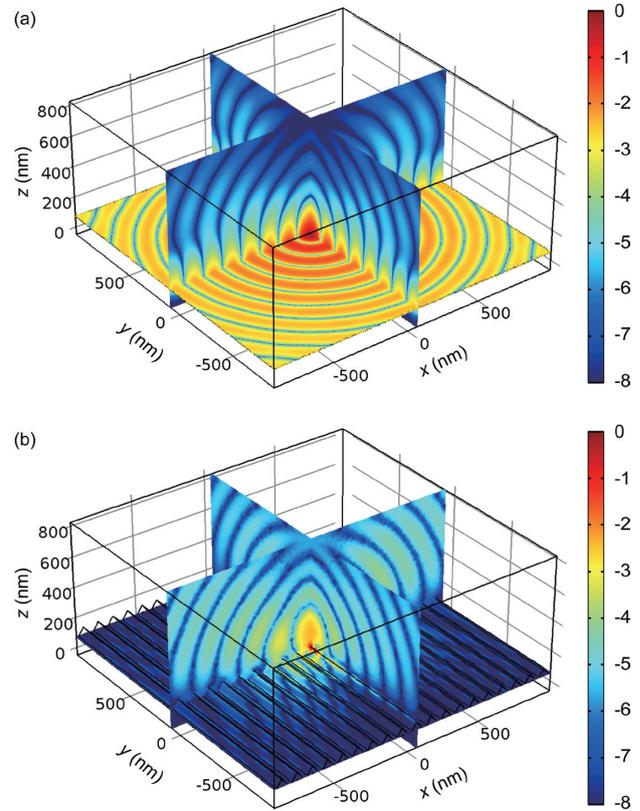

Fig. 4 3D simulated field distribution of a dipole emission in a 2-layer structure with (a) flat, and (b) nanograting interface. The field intensity is normalized and plotted on a log color scale.

The mathematical formulations can be summarized as follows:

$$P_{total} = \int (\vec{E} \times \vec{H}) \cdot d\vec{S_0} \qquad (1)$$

$$P_{light} = \int (\vec{E} \times \vec{H}) \cdot d\vec{S_1} \qquad (2)$$

$$P_{plasmon} = \int (\vec{E} \times \vec{H}) \cdot d\vec{S_2} + \int (\vec{J} \times \vec{E}) \cdot dV_{Ag} \qquad (3)$$

A percentage of plasmon loss then can be estimated by $P_{plasmon}/P_{total}$.

Fig. 5 plots the percentage of plasmon loss for a flat and a nanograting structure as a function of the vertical distance between the dipole source and the interface calculated for P_y at 535 nm with $\Delta_x = 0$ and the grating with $\lambda_G = 300$ nm, $L = 150$ nm, $h = 50$ nm. The result indicates that significant reduction of plasmon loss can be achieved with the nanograting structure when the distance between the dipole and the interface is less than about 100 nm, e.g., a maximum

of over 50% reduction at $d = 60$ nm (**Fig. 5**). As the distance further increases, the plasmon loss of the flat structure decreases to insignificant level, while that of the nanograting remains at around 40%, inferior to the flat structure. This observation is in agreement with the previous studies[3], suggesting that the nanograting cathode is useful for reducing plasmon loss only if the separation of the emission layer from the cathode is within about hundred nanometers.
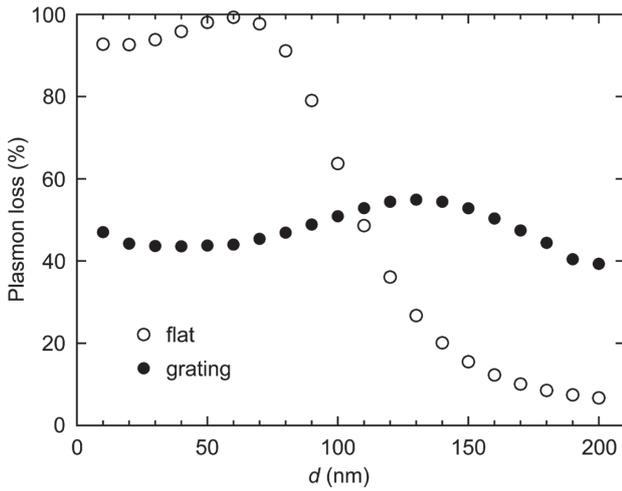

Fig. 5 Percentage of plasmon loss for a 2-layer structure as a function of the distance of the dipole from the layer interface.

3.5 Parametric study

Extensive parametric sweeps were performed to explore the dependence of the plasmon loss on a number of factors such as the dipole position (d, Δ_x), dipole orientation (P_x, P_y), emission wavelength (λ_0), and the grating size and shape (λ_G, L, h), etc. Detailed analysis of the parametric study is beyond the scope of this article. Here we give one example on the grating structural optimization. **Fig. 6 (a)** presents a 2D map of the relative ratio of plasmon loss (the grating with respect to the flat) as a function of two grating geometrical parameters, the pitch height (h) and the pitch duty ratio (L/λ_G), for a given grating period ($\lambda_G = 100$ nm) and vertical position of the dipole ($d = 50$ nm). The data are averaged over 2 dipole orientations (P_x and P_y), 2 horizontal dipole positions ($\Delta_x = 0$ and $\Delta_x = \lambda_G/2$), and 3 emission wavelengths ($\lambda_0 = 475$ nm, 535 nm, and 625 nm). It evaluates the overall plasmon reduction effect of the grating structure; the smaller the relative ratio (i.e. darker the color in **Fig. 6 (a)**), the larger the reduction. **Fig. 6 (b)** plots the corresponding standard deviation from the wavelength averaging, which provides a rough estimation on its broadband performance. A smaller value

indicates more uniform performance across the three different wavelengths. Thus common dark cells in **Fig. 6 (a)** and **Fig. 6 (b)** would indicate the optimal structural configurations for plasmon loss reduction. For example, the cell marked by a dashed circle has a relative ratio of 0.37 and a standard deviation of 0.09, or 0.37 ± 0.09, suggesting that ~50% reduction of plasmon loss over a broadband emission is promising by optimized grating cathode structures.
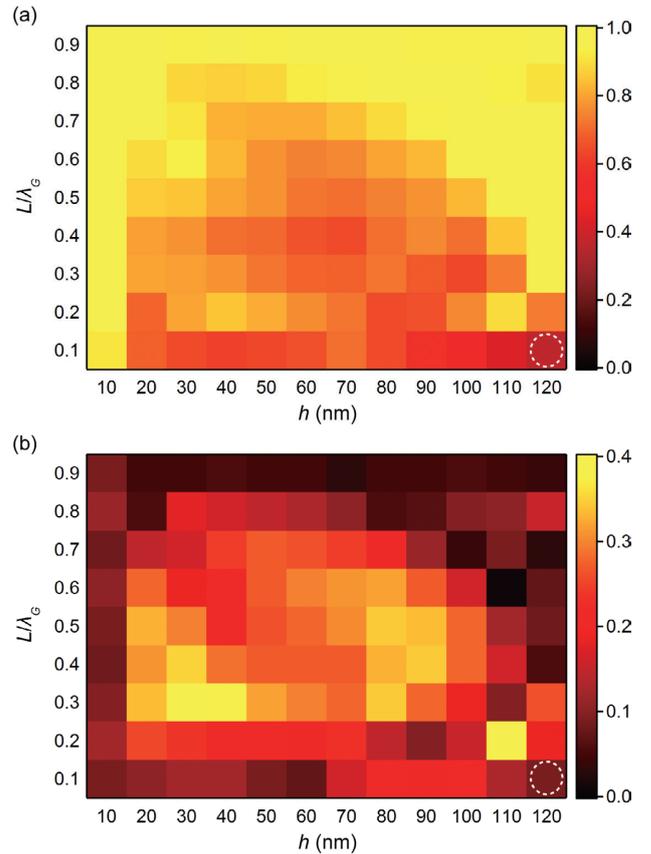

Fig. 6 (a) Averaged relative plasmon loss of a nanograting with respect to a flat cathode structure as function of grating pitch height and duty ratio, and (b) the corresponding standard deviation in wavelength averaging. In (a), the color is saturated at 1.

4 Summary

We have developed a FEM numerical model to simulate light field distribution and plasmon effect in OLED, and applied it to evaluate possible plasmon reduction by nanograting-structured cathode. The FEM model allows simulation of the optical effect caused by arbitrary subwavelength structures which is usually incapable to achieve with analytical simulations. Our simulation results suggest that significant reduction of plasmon energy loss over a broadband emission is promising by optimized metal cathode structures, providing a valuable reference for future experimental development.

5 Acknowledgement

Reference

1) K. Hong, and J. -L. Lee, Review paper: recent developments in light extraction technologies of organic light emitting diodes, *Electronic Materials Letters*, **7**, 77-91 (2011)
2) J. Frischeisen, D. Yokoyama, A. Endo, C. Adachi, and W. Brütting, Increased light outcoupling efficiency in dye-doped small molecule organic light-emitting diodes with horizontally oriented emitters, *Organic Electronics*, **12**, 809-817 (2011)
3) S. Nowy, J. Frischeisen, and W. Brütting, Simulation based optimization of light-outcoupling in organic light-emitting diodes, *Proc. of SPIE*, **7415**, 7415C (2009)
4) J.-B. Kim, J.-H. Lee, C.-K. Moon, S.-Y. Kim, and J.-J. Kim, Highly enhanced light extraction from surface plasmonic loss minimized organic light-emitting diodes, *Advanced Materials*, **25**, 3571-3577 (2013)
5) J. Frischeisen, Q.Niu, A. Abdellah, J. B. Kinzel, R. Gehlhaar, G. Scarpa, C. Adachi, P. Lugli, and W. Brütting, Light extraction from surface plasmons and waveguide modes in an organic light-emitting layer by nanoimprinted gratings, *Optics Express*, **19**, A7-A19 (2011)
6) L. Zschiedrich, H. J. Greiner, S. Burger, and F. Schmidt, Numerical analysis of nanostructures for enhanced light extraction from OLEDs, *Proc. of SPIE*, **8641**, 8641B (2013)
7) A. Chutinan, K. Ishihara, T. Asano, M. Fujita, and S. Noda, Theoretical analysis on light-extraction efficiency of organic light-emitting diodes using FDTD and mode-expansion methods, *Organic Electronics*, **6**, 3-9 (2005)
8) P. B. Johnson, and R. W. Christy, Optical constants of the noble metals, *Physical Review B*, **6**, 4370-4379 (1972)
9) J. E. Sipe, The dipole antenna problem in surface physics: a new approach, *Surface Science*, **105**, 489-504 (1981)

Source